

Efficient Directional Coupling between Silicon and Copper Plasmonic Nanoslot Waveguides: toward Metal–Oxide–Silicon Nanophotonics

Cécile Delacour,^{*,†} Sylvain Blaize,[†] Philippe Grosse,[†] Jean Marc Fedeli,[†] Aurelien Bruyant,[‡] Rafael Salas-Montiel,[†] Gilles Lerondel,[†] and Alexei Chelnokov^{*,†}

[†]CEA, LETI, MINATEC, DOPT 17 rue des martyrs 38054 Grenoble cedex 9, France, and [‡]Laboratoire de Nanotechnologie et d'Instrumentation Optique, Institut Charles Delaunay, CNRS-FRE 2848, Université de Technologie de Troyes, BP 2060, 10010 Troyes, France

ABSTRACT Coupling plasmonics and silicon photonics is the best way to bridge the size gap between macroscopic optics and nanodevices in general and especially nanoelectronic devices. We report on the realization of key blocks for future plasmonic planar integrated optics, nano-optical couplers, and nanoslot waveguides that are compatible both with the silicon photonics and the CMOS microelectronics. Copper-based devices provide for very efficient optical coupling, unexpectedly low propagation losses and a broadband sub-50 nm optical confinement. The fabrication in a standard frontline microelectronic facilities hints broad possibilities of hybrid opto-electronic very large scale integration.

KEYWORDS Surface plasmon polariton, metallic slot waveguides, codirectional couplers, silicon photonics, plasmonics, integrated optics.

Being very compact,^{1–3} plasmonic waveguides should provide for efficient optical coupling to truly nanoscopic devices.⁴ They can guide both light and electrical current. In addition, high optical confinement can significantly decrease the threshold of nonlinear effects for all-optical switching applications.⁵

To be widely used, the plasmonic technology should fulfill three requirements. First, interfaces to the outside microscopic world should be efficient. Accordingly, operation in the near IR wavelength range (1.3–1.55 μm) and coupling to standard single mode optical fiber is preferred. Second, the small size of the unitary device is of no big benefit if the plasmonic devices are not highly integrated with similar devices or with electronic integrated circuits. Therefore, planar-guided integration is obviously preferable. Finally, the integration with silicon photonics^{6–8} and with electronics¹¹ implies full technological compatibility with the mainstream CMOS front end fabrication.

In this paper, we show that highly efficient plasmonic waveguides and nonresonant optical couplers between metallic and silicon optical waveguides can be achieved in a fully CMOS-compatible way.

Single-mode silicon ridge waveguides with cross section of 220 nm by 400 nm are now standard in silicon photonics. Efficient coupling with standard optical fibres is readily obtained using either grating⁹ or inverted taper couplers.¹⁰

Here we choose to explore metallic slotline waveguides that can be traced back to the microwave domain^{12,13} in the near-IR and to couple them to the standard silicon ridge waveguides. The slotline configuration appears to be the most promising since it can be fabricated using a single lithography step. Compared to a stripline waveguide, the optical field is strongly confined inside the slot with very little outside spreading. The guiding side parts can act as contact electrodes to implement opto-electrical devices.^{14,15} Moreover, the slotline mode has the same symmetry^{16,17} as the fundamental mode of the silicon waveguide and the appropriate polarization.

Compared to the microwave domain, slotlines at optical wavelengths are proportionally thicker. However their operation still should be efficient in a very large wavelength range. Simulations¹⁸ have predicted the mode sizes down to 50 nm by 50 nm in the NIR domain with 10 μm of surface plasmon propagation length for noble metals such as silver.

Because of much smaller size of the guided plasmonic mode, butt coupling to the Si waveguides would have had a prohibitively low efficiency. Nonresonant butt coupling was shown numerically to be possible only for infinitely large plasmonic waveguides and slab dielectric waveguides.¹⁹ For transversely confining metallic waveguides, numerical modeling suggested either narrow band resonant structures similar to RF antennas or tapered mode adapters that are however complex to fabricate.^{20,21}

We choose here to use directional coupling^{22,23} between Si and metallic slotline waveguides, both of constant cross section. The principle of directional coupling between two waveguides is widely known and used.²⁴ The directional

* To whom correspondence should be addressed. E-mail: (C.D.) cecile.delacour@cea.fr; (A.C.) alexei.chelnokov@cea.fr.

Received for review: 03/26/2010

Published on Web: 07/19/2010

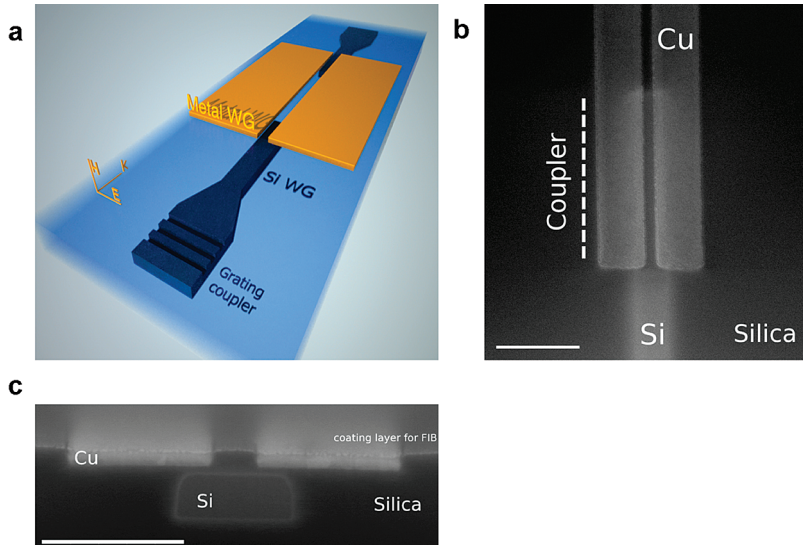


FIGURE 1. Hybrid optical chip. (a) Art picture of the hybrid optical chip showing the metallic slotline coupled to silicon ridge waveguides. Slotline consists in two coplanar metallic strips spaced to form the dielectric slot. The metallic and silicon waveguides are vertically spaced. Coupling occurs at the overlapping area. A diffraction grating is used to couple the light from an optical fiber to the silicon waveguide in the spectral range of 1.3 to 1.6 μm . (b) Scanning electron micrograph of the input coupler. The coupling area underlined by the dashed line is clearly identified due to the underneath silicon ribbon leading to higher secondary electron emission rate. Scale bar is 1 μm . (c) Scanning electron micrograph of the coupler cross-section showing the adjacent copper and silicon waveguides vertically spaced by silica (typ. 30 nm). Scale bar is 500 nm.

couplers are nonresonant and highly efficient despite fabrication imperfections.

The plasmonic photonic hybrid structure studied in this paper is shown in the Figure 1. It includes a plasmonic slotline waveguide (Figure 1a–c) composed of two copper strips separated with a nanoscale slot. The slotline waveguide is in a close vicinity of an interrupted silicon ridge monomode waveguide with two overlapping areas respectively for front and back end coupling. The whole structure is embedded in silica. The overlapping area in the direction of the propagation defines the coupling length over which energy power exchange between the two waveguides is expected to occur.

In the overlapping area, the two coupled waveguides form a superstructure (i.e., a waveguide composed of two adjacent waveguides regarded as one) supporting two guided supermodes (i.e., eigenmodes of the superstructure) of even (e) and odd (o) symmetries. The supermodes result from the coupling of the two primary original photonic and plasmonic modes (Figure 2). The propagation constants of the supermodes being different, the power exchange between the WGs can be represented as a beating between these two supermodes.

The overlap of the original guided modes and thus the strength of their interaction can be represented through a coupling constant (κ). The fraction of exchanged power and the coupling length (L_c) are function of both the phase velocity mismatch (δ) and the coupling constant. In a strong coupling regime defined as ($\delta/\kappa \ll 1$), short coupling length, and high fraction of exchanged power can be achieved (see Supporting Information).

The plasmonic couplers we build operate in the strong coupling regime. The plasmonic mode is strongly confined inside the slot, so in order to get strong optical coupling the guides should be placed in a very close vicinity, typically several tens of nanometers (Figure 2b), while keeping the phase velocity mismatch as small as possible ($\delta \sim 0$).

It happens that in the strong coupling, each supermode carries half of the total power, so that due to the interference between the supermodes an almost total transfer of power from one waveguide to another on the characteristic period of $2L_c$ is expected (see Supporting Information).

The electrical field in the superstructure is illustrated in the Figure 2c. An extremely short beating length of less than one free-space wavelength ($L_c = 1 \mu\text{m}$) combined with a high coupling efficiency (75% of the electrical field amplitude) confirm a strong coupling between the guided modes ($\kappa = 1256 \text{ mm}^{-1}$). This value has to be compared with this of all-dielectric couplers²⁵ (typ. $L_c = 100 \mu\text{m}$).

We fabricated the devices in a 200 mm wafer CMOS front end fabrication facility using 193 nm optical projection lithography and metals that are non contaminant for the Si microelectronics (see Supporting Information). All the experimental results reported in the present paper are obtained with copper.

It is known that the roughness and the granularity of the metals strongly impede the propagation of plasmonic modes.²⁶ To significantly improve the nanoscopic quality of the metal surface in contact with the light field in the slotline, a modified Damascene technology was developed. The propagation losses should be strongly reduced compared to those obtained with conventional lift-off, focused ion beam,

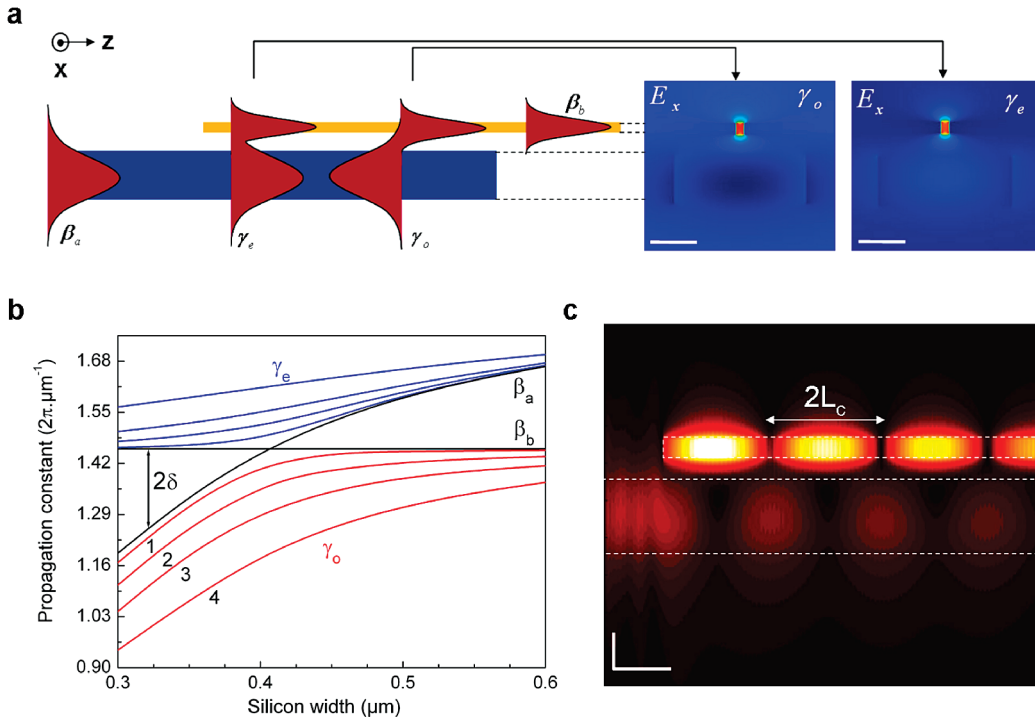


FIGURE 2. Proof of concept. (a) Schematic view of the guided modes in the hybrid structure. Propagation constant of the pure photonic and plasmonic modes are respectively denoted ($\beta_{a,b}$) in the uncoupled area. In the superstructure, ($\gamma_{e,o}$) respectively, denote the propagation constant of the even and odd supermodes. Right: Simulated ex-electrical field amplitude of each supermode in a coupler formed for this example by a silver slotline ($25 \times 50 \text{ nm}^2$) and the silicon ($w \times 220 \text{ nm}^2$). Incident wavelength is $\lambda_0 = 1.55 \mu\text{m}$ and the scale bar is 200 nm. (b) Modal analysis of the coupler. Propagation constant of both local (black curves) and supermodes (red and blue curves) are reported as function of the silicon width (showing the velocity phase matching dependence) and for several spacing (showing the coupling strength dependence). For the curves numbered 1 to 4, the spacing is varied from 50 to 200 nm, respectively. (c) Interference pattern of the electrical field (square of the amplitude) resulting from the interaction of the even and odd supermodes in the superstructure at the phase velocity matching condition. Period of modulation is denoted $2L_c$ and was found here to be $2.5 \mu\text{m}$. A monochromatic source is used with $\lambda_0 = 1.55 \mu\text{m}$. Horizontal and vertical scale bars are respectively of 1 and $0.1 \mu\text{m}$.

or direct metal etching processes. Each fabricated device includes a slotline metallic waveguide, two directional Si-to-Cu couplers and two optical fiber grating couplers (Figure 1a). Please note that outside of the directional couplers themselves, the silicon waveguide is absent under the slotline metallic waveguide and that the light can be guided only by the slotline.

The transmission of the devices was measured around the wavelength of $1.55 \mu\text{m}$ using both wide band superluminescent light emitting diodes (SLED) and a laser, all interfaced via monomode fibres. Since the metallic slotlines support only TE polarized mode, we report only the measurements for this polarization. The data were normalized with respect to the transmission of a continuous 400 nm wide silicon waveguide. For each device with a slotline, an identical device but without a metallic slotline was fabricated side by side with the former. The transmission of this second device (i.e., a narrow Si WG cut in the middle by $6 \mu\text{m}$), corresponding to the case when no light is coupled to the slotline, was very small, typically 2 %. Nevertheless, it was systematically retrenched from the transmission values.

The SLED measurements confirmed the wide nonresonant spectral operation of the structures. The Figure 3b shows the modulation of the monochromatic transmission

intensity as function of the coupling length between the silicon and the copper slotline waveguides, for several widths of silicon waveguide. The predictions from the codirectional coupling model are used as a guide to the eye with the dimensions taken as the dimensions targeted during the fabrication processing. Experimental data (squares) confirm the oscillatory shape of the efficiency versus overlapping length predicted by the codirectional coupling model (solid lines).

For the optimized configuration, very high “silicon–slotline–silicon” transmissions of 50 % or more have been measured suggesting lower than expected propagative loss of the plasmonic mode in the $6 \mu\text{m}$ long slotline. Such a value is obtained for a Cu waveguide with a metal–silicon gap of 30 nm , overlapping by $0.9 \mu\text{m}$ the 400 nm wide Si waveguide (Figure 1c). At the same time, the measured overall transmissions yield in at least 70 % coupling efficiency of each directional coupler (even if we consider zero loss of the Cu slotline, which is not true). Such an efficient coupling is the direct consequence of the strong coupling constant ($\kappa = 1900 \text{ mm}^{-1}$) between the plasmonic and the dielectric waveguide modes. We explain the reasonably small discrepancy between the model and the measurements that is observed for the smallest coupling lengths ($< 1 \mu\text{m}$) as a result

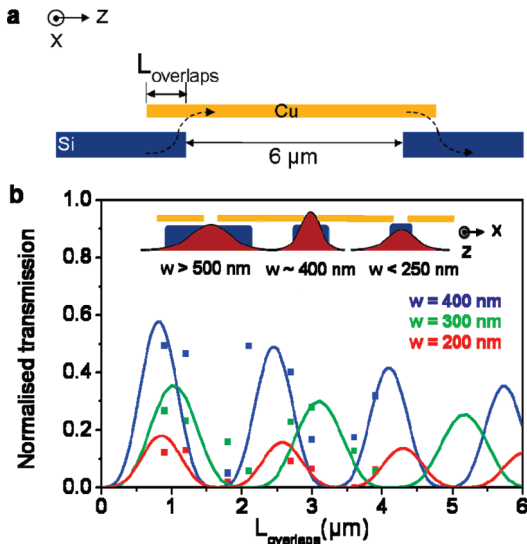


FIGURE 3. Coupler–slotline–coupler transmissions. (a) Schematic view of the hybrid structure showing the device setup. (b) Normalized transmission as function of the overlapping length and for several silicon widths (400, 300, 200 nm). Experimental data (squares) are normalized with respect to the transmission of a continuous 400 nm wide silicon waveguide and the transmission of structure identical with the studied one but without the copper slotline (typ. 2%). The solid lines are guides to the eye corresponding to the predictions of the coupled mode model added with potential losses from the 6 μm copper slotline connecting the couplers (see Supporting Information). On the top is reported a schematic cross section of the photonic mode as function of the silicon waveguide width. Laser source is $\lambda_0 = 1.55 \mu\text{m}$. The targeted slotline width is 100 nm.

of fabrication imperfections. Numerical simulations supported by our separate experiments suggest that the discrepancy is decreased and the overall coupling is fairly improved by finely tuning the separation between the two waveguides.

The reported numbers have been obtained on a very large number of tested couplers/waveguides. Example of statistics realized on 575 optimized devices is shown on Supporting Information Figure 1a. At the fixed wavelength of 1.55 μm , 30% of the tested devices exhibit a silicon–slotline–silicon transmission above 40%. We assume that statistical dispersion is mainly due to the variation in the two waveguides spacing as defined by chemical mechanical polishing. The thickness of the silica spacer can vary from almost 0 to 50 nm over the entire 200 mm wafer.

To confirm the results of macroscopic characterisations, we analyzed the operation of the couplers/guides combinations at a wavelength scale using transmission-based near-field scanning optical microscope operating at 1.55 μm .

The intensity of the optical near-field reported in Figure 4b clearly shows the surface plasmon polariton supported by the metal–dielectric–metal interfaces inside the slotline. Modulation of the intensity occurs with a period of 420 nm, suggesting the reflection of the uncoupled light at the ends of the slot in agreement with an effective index of the surface plasmon of about 1.85. This very interesting

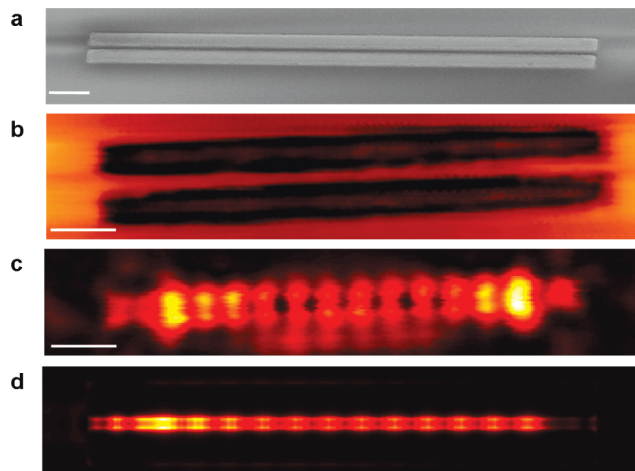


FIGURE 4. Near-field characterization. (a) Scanning electron micrograph of a copper slotline showing the two coplanar copper strips spaced by the silica slot. (b) Scanning atomic force micrograph of a copper slotline coupled to the buried silicon (typ. 200 \times 400 nm^2) waveguide. Coupling length is 0.9 μm . Metal–silicon gap is 30 nm (Figure 1c). (c) Optical near-field micrograph clearly shows the plasmonic mode confined in the slot. The two brightest regions correspond to the input and output coupling to the silicon waveguides. Magnitude of the field oscillates along the propagation direction with a period of 420 nm. The silicon waveguides are buried so their signal is lower. (d) Numerical simulation (FDTD) of the tested device showing the steady state of the energy density of the electrical field. For both measurement and simulation a monochromatic source of $\lambda_0 = 1.55 \mu\text{m}$ was used. Scale bars are 1 μm .

result underlines the low loss of the copper waveguide. Optical and material properties of the high quality copper film are currently further investigated. The signal related to the photonic mode of the Si waveguide is weaker than that of the Cu waveguide, as the silicon waveguide is embedded much deeper into the silica. Our simulations of the tested device (Figure 4c) predict that almost 60% of incident power is transmitted to the output waveguide with monochromatic source at 1.55 μm in agreement with experimental data (Figure 3b, Supporting Information Figure S1a).

In conclusion, we have demonstrated highly efficient plasmonic devices technologically compatible with both Si photonics and Si electronics. The two most essential bricks of plasmonic integrated optics (waveguide and coupler) were integrated with traditional silicon photonic waveguides and operated at the optical telecommunications wavelengths. Slotline waveguides and couplers do potentially convey both the light and the electrical current and can therefore bridge the size gap between the nanodevices and the macroscopic world represented by single-mode optical fiber. The present demonstration enables more complex integrated plasmonic devices as the already suggested plasmonic based modulators^{14,27,29–32} and sources.^{7,28}

Acknowledgment. We acknowledge K. Gilbert, N. Olivier and G. Rabillé for technical contributions regarding fabrication and characterization. The samples used in the investigations were made in the clean rooms of CEA LETI. This work

was partially financed by the French National Research Agency (ANR) through Carnot funding.

Supporting Information Available. Device fabrication, on-wafer statistics of the device performances, recall of directional coupling principle, and details of the numerical modeling and of the SNOM measurements. This material is available free of charge via the Internet at <http://pubs.acs.org>.

REFERENCES AND NOTES

- (1) Zia, R.; Schuler, J. A.; Chandran, A.; Brongersma, M. L. Plasmonics: the next chip-scale technology. *Mater. Today* **2006**, *9*, 20–27.
- (2) Ozbay, E. Plasmonics: merging photonics and electronics at nanoscale dimensions. *Science* **2006**, *311*, 189–193.
- (3) Barnes, W. L.; Dereux, A.; Ebbesen, T. W. Surface plasmon subwavelength optics. *Nature* **2003**, *424*, 824–30.
- (4) Akimov, A. V.; et al. Generation of single optical plasmons in metallic nanowires coupled to quantum dots. *Nature* **2007**, *450*, 402–406.
- (5) Koos, C.; et al. All-optical high-speed signal processing with silicon-organic hybrid slot waveguides. *Nat. Photonics* **2009**, *3*, 216–219.
- (6) Chen, L.; Shakya, J.; Lipson, M. Subwavelength confinement in an integrated metal slot waveguide on silicon. *Opt. Lett.* **2006**, *31*, 2133–2135.
- (7) Walters, R. J.; et al. A silicon-based electrical source of surface plasmon polaritons. *Nat. Mater.* **2010**, *9*, 21–25.
- (8) Dionne, J. A.; et al. Silicon-based plasmonics for on-chip photonics. *IEEE J. Sel. Top. Quantum Electron.* **2010**, *16*, 295–306.
- (9) Roelkens, G.; et al. High efficiency diffractive grating couplers for interfacing a single mode optical fiber with a nanophotonic silicon-on-insulator waveguide circuit. *Appl. Phys. Lett.* **2008**, *92*, 131101.
- (10) Almeida, V. R.; Panepucci, R. R.; Lipson, M. Nanotaper for compact mode conversion. *Opt. Lett.* **2003**, *28*, 1302–1304.
- (11) Mekis, A.; et al. Monolithic integration of photonic and electronic circuits in a CMOS process. *Proc. SPIE* **2008**, *6897*, L1–14.
- (12) Gupta, K. C.; Garg, R.; Bahl, I.; Bhartia, P. *Microstrip Lines and Slotlines*; Artech house: Boston, 1996.
- (13) Cohn, S. B. Slot line on a dielectric substrate. *IEEE Trans. Microwave Theory Tech.* **1969**, *MTT-17*, 768–778.
- (14) Cai, W.; White, J. S.; Brongersma, M. Compact, high-speed and power-efficient electrooptic plasmonic modulator. *Nano Lett.* **2009**, *9*, 4403–4411.
- (15) Cohen, G. M.; et al. Nanowire metal-oxide-semiconductor field effect transistor with doped epitaxial contacts for source and drain. *Appl. Phys. Lett.* **2007**, *90*, 233110.
- (16) Economou, E. N. Surface plasmon in thin films. *Phys. Rev.* **1969**, *182*, 539–554.
- (17) Dionne, J. A.; Sweatlock, L. A.; Atwater, H. A. Plasmon slot waveguides: towards chip-scale propagation with subwavelength-scale localization. *Phys. Rev. B* **2006**, *73*, 035407.
- (18) Veronis, G.; Fan, S. Guided subwavelength plasmonic mode. *Opt. Lett.* **2005**, *30*, 3359–3361.
- (19) Veronis, G.; Fan, S. Theoretical investigation of compact couplers between dielectric slab waveguides and two-dimensional metal-dielectric-metal plasmonic waveguides. *Opt. Express* **2007**, *15*, 1211–1221.
- (20) Ginzburg, P.; Arbel, D.; Orenstein, M. Gap plasmon polariton structure for very efficient microscale-to-nanoscale interfacing. *Opt. Lett.* **2006**, *31*, 3288–3290.
- (21) Feigenbaum, E.; Orenstein, M. Modeling of complementary (void) plasmon waveguiding. *J. Lightwave Technol.* **2007**, *25*, 2547–2562.
- (22) Yariv, A. Coupled-mode theory for guided-wave optics. *J. Quantum Electron.* **1973**, *9*, 919–933.
- (23) Huang, W. P. Coupled-mode theory for optical waveguides: an overview. *J. Opt. Soc. Am. A* **1994**, *11*, 963–983.
- (24) Gramotnev, D. K.; Vernon, K. C.; Pile, D. F. P. Directional coupler using gap plasmon waveguides. *Appl. Phys. B* **2008**, *93*, 99–106.
- (25) Sun, X. K.; Liu, H. C.; Yariv, A. Adiabaticity criterion and the shortest adiabatic mode transformer in a coupled-waveguide system. *Opt. Lett.* **2009**, *34*, 280–282.
- (26) Diltbacher, H.; et al. Silver Nanowires as surface plasmon resonators. *Phys. Rev. Lett.* **2005**, *95*, 257403.
- (27) Dionne, J. A.; et al. Plasmotor: a metal oxide Si field effect plasmonic modulator. *Nano Lett.* **2009**, *9*, 897–902.
- (28) Hryciw, A.; Jun, Y. C.; Brongersma, M. L. Plasmonics: Electrifying plasmonics on silicon. *Nat. Mater.* **2010**, *9*, 3–4.
- (29) Pacifici, D.; Lezec, H. J.; Atwater, H. A. All-optical modulation by plasmonic excitation of CdSe quantum dots. *Nat. Photonics* **2007**, *1*, 402–406.
- (30) Pala, R. A.; Shimizu, K. T.; Melosh, N. A.; Brongersma, M. L. A nonvolatile plasmonic switch employing photochromic molecules. *Nano Lett.* **2008**, *8*, 1506–1510.
- (31) Dicken, M. J.; Sweatlock, L. A.; Pacifici, D.; Lezec, H. J.; Bhattacharya, K.; Atwater, H. A. Electrooptic modulation in thin film barium titanate plasmonic interferometers. *Nano Lett.* **2008**, *8*, 4048–4052.
- (32) MacDonald, K. F.; Samson, Z. L.; Stockman, M. I.; Zheludev, N. I. Ultrafast active plasmonics. *Nat. Photonics* **2008**, *3*, 55–58.